Table 1. Composition ratio and thickness of PMMA SPE film prepared

ID	Weight Percentage wt%				
	PMMA	EC	$LiCF_3SO_3$	Al_2O_3	SiO_2
SPE1	55	18	25	-	-
SPE2	55	18	25	2 (≤10μm)	-
SPE3	55	18	25	-	2 (≤10μm)

2.2 ELECTROCHEMICAL IMPEDANCE SPECTROSCOPY (EIS)

Electrochemical Impedance Spectroscopy (EIS) was carried out using Gamry reference 600 series potentiostat for frequency ranging from 0.1Hz to 1MHz at room temperature with the sample sandwiched between two spring-loaded stainless-steel electrodes. The ionic conductivity is calculated by using the following equation:

$$\sigma = \frac{t}{R_B A} \tag{1}$$

, where t (cm) is the thickness of SPE film, R_B is the bulk resistance of electrolyte obtained from the Nyquist plot, and A (cm^2) is the contact area between the film and the electrode, which equates to 2.56 cm^2 in this work. The results of PMMA SPE ionic conductivity were tabulated in Table 2.

2.3 TRANSFERENCE NUMBER CHARACTERISATION

The lithium transference number was defined as the number of moles of lithium-ion transferred for one Faraday of charge transferred. Ideally, the lithium transference number should be close to one in a high conductivity lithium polymer battery, and the lithium transference number, t^+ is calculated as:

$$t^+ = \frac{I_s}{I_o} \tag{2}$$

where I_o and I_s represent the initial and steady-state cell currents, respectively, however, the existing system is more complicated, with minute traces of contaminant of oxidation on the electrodes that can alter the experiment results. Hence Bruce *et al.* [12] introduced a correction factor to characterize the system before and after polarization, and the equation was rewritten as:

$$t^+ = \frac{I_s(\Delta V - I_o R_o)}{I_o(\Delta V - I_s R_s)} \tag{3}$$

ΔV is the polarization voltage of 20mV, R_o and R_s are the bulk resistance of electrolytes film taken into account interfacial resistance before and after the polarization, respectively (Bruce, 1987). Thus, the electrolyte film was characterized using EIS before and after dc polarization to determine the initial resistance, R_o, and the steady-state resistance, R_s of the sample (Pozyczka, 2017).

The Bruce-Vincent method is a reliable technique employed by multiple researchers to obtain lithium transference numbers in the polymer electrolytes system (Pozyczka, 2017; Yang, 2019; Xiao, 2018). High interfacial resistance was always the factor in limiting the performance of SPEs. Multiple researchers have reported that interfacial resistance was caused by the deposition of the oxide layer resulting from the diffusion of non-lithium ions during the chemical reaction. Besides, poor contact between the electrode and electrolytes interface, originating from the two different materials mismatched lattice and the volume changes occurring during cycling also increase the interfacial resistance (Ding, 2020; Jiang, 2019).

2.4 VOLTAMMETRY AND DISCHARGING TEST

Linear Sweep Voltammetry (LSV) was used to investigate the electrochemical stability window of SPEs. The potential window, representing the sample stability voltage, is a critical parameter that has to be evaluated to determine the application voltage used in electrochemical devices (Aziz, 2019). The voltage was swept from 0V (versus stainless steel electrode) at a scan rate of $5mVs^{-1}$ until the breakdown of electrolyte films (sharp increment of current) to determine the electrochemical stability voltage of the samples.

Then, five cycles of cyclic voltammetry (CV) were performed on the SPE film from 0V to 3V at a scan rate of 20 mVs^{-1}, in which the SPE film was sandwiched between two stainless steel electrodes. Lastly, the SPE film was then assembled to evaluate its discharge performance. The cell was discharged with a current of 0.01mA at room temperature from 2V to 0.1V using stainless steel electrodes. All the measurements were carried out using a Gamry Reference 600 series potentiostat.

3.0 RESULTS AND DISCUSSION

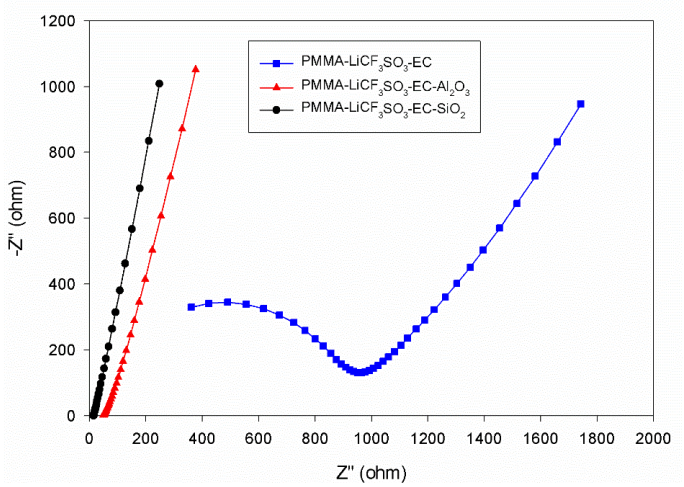

Figure 1. Nyquist plot of PMMA-$LiCF_3SO_3$-EC (Square), PMMA-$LiCF_3SO_3$-EC-Al_2O_3 (Triangle), and PMMA-$LiCF_3SO_3$-EC-SiO_2 (Circle).

Table 2. Ionic conductivity of PMMA-based solid polymer electrolytes.

Sample ID	Sample Composition	Filler	Filler Size	Ionic conductivity (S/cm)
SPE1	PMMA-$LiCF_3SO_3$-EC	-	-	1.22×10^{-5}
SPE2	PMMA-$LiCF_3SO_3$-EC-Al_2O_3	Al_2O_3	10 μm	1.83×10^{-4}
SPE3	PMMA-$LiCF_3SO_3$-EC-SiO_2	SiO_2	10 μm	2.35×10^{-4}

Figure 1. shows the Nyquist plot for SPE1, SPE2, and SPE3, respectively (see Figure 1). The appearance of semicircle for SPE1 suggests the presence of bulk capacitance in the system. Simultaneously, the linear line adjacent to the semicircle indicates the diffusion process resulting in electrode polarization effect (Saikia, 2008; Sivakumar, 2015). Furthermore, no semicircle is observed for SPE2, and SPE3 suggests only resistive components prevail.

The value of bulk resistance was determined at the interception point between the Nyquist curve and the x-axis, which corresponds to 964 Ω, and the obtained ionic conductivity is shown in Table 2. Ionic conductivity calculated for SPE1 was 1.22×10^{-5} S/cm. In comparison, Pal *et al.* obtained ionic conductivity of 3.52×10^{-5} S/cm for plasticized PMMA-$LiClO_4$ SPEs (Pal, 2018). Kurapati *et al.* also reported ionic conductivity values of 8.21×10^{-5} S/cm for her study on PMMA-CH_3COOLi SPEs (Kurapati, 2019). The obtained ionic conductivity for SPE1 was too low for electrochemical device applications (Chauvin, 2006). The low ionic conductivity of SPEs is the attribute of their crystalline nature, where the ionic mobility is low. Besides that, most of the Li^+ ions already formed polymer-salt complexes with the polymer, reducing the fraction of ions available for ionic conduction.

Improvement in ionic conductivity was seen for SPE2 and SPE3 when inorganic fillers Al_2O_3 and SiO_2 of (≤10μm) were added, yielding an ionic conductivity of 1.83×10^{-4} S/cm and 2.35×10^{-4} S/cm, respectively. Chew *et al.* reported similar findings where they also observed improvement in ionic conductivity when they added Al_2O_3 into PMMA SPEs (Chew, 2011). They obtained an ionic conductivity of 2.05×10^{-4} S/cm for PMMA SPEs with Al_2O_3 fillers, an improvement from 1.36×10^{-5} S/cm without inorganic fillers. Marcinek *et al.* explained that the improvement in ionic conductivity was associated with the increases in conduction pathways for ionic conduction provided by inorganic filler due to their larger surface area (Marcinek, 2000).

Besides that, the presence of inorganic particles in the polymer matrix also lowers the fraction of polymer-salt complexes, which increases the fraction of Li^+ ions free for ionic conduction. Saikia et al. (Saikia, 2008) reported that the glass transition temperature (T_g) and crystallinity of P(VDF-HFP)-PC-$LiClO_4$ decreases from -98˚C to -104.6˚C with the addition of 4 wt% SiO_2 aerogel particles. In Addition, Pitawala also reported decreases in *Tg* from -44˚C to -49˚C when they added 10 wt% of Al_2O_3 fillers into $(PEO)_9LiTf$ Furthermore, Dissanayake *et al.* also reported that the presence of inorganic fillers promotes amorphous region in the polymer matrix by lowering the transition temperature (Dissanayake, 2003). But they also informed that higher filler concentration above its optimal level would impose geometrical constriction, lowering the ion mobility. They reported 15 wt% of inorganic filler provided the maximum enhancement. Furthermore,

another study conducted by Yang *et al.* (Yang, 2010) show that decreases in conductivity with increasing filler content beyond 2.5 wt% attributed to an aggregation of fillers, strongly impeding polymer chain movement.

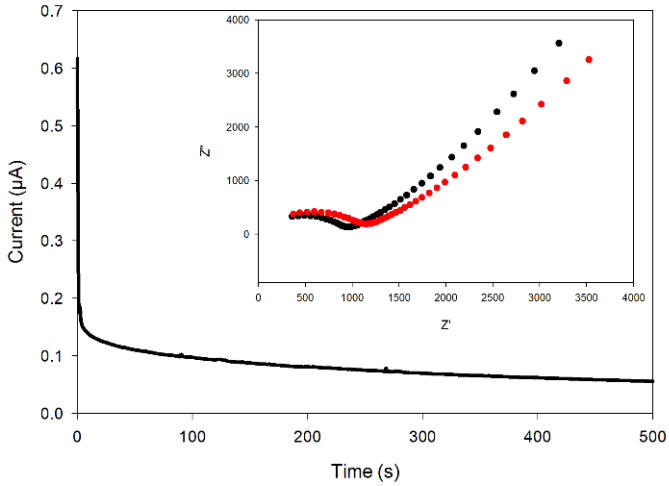

Figure 2. DC Polarization curve obtained via chronoamperometry for PMMA-$LiCF_3SO_3$-EC (SPE1) samples. (Inset Nyquist curve of SPE1 before and after dc polarization)

Table 3. Transference number of PMMA-based polymer electrolytes.

Sample ID	Io (μA)	Is (μA)	R_o (Ω)	R_s(Ω)	t^+
SPE1	0.617	0.055	964.1	1159	0.088
SPE2	0.834	0.180	69.42	75.31	0.215
SPE3	1.010	0.266	51.63	81.25	0.263

Figure 2. shows the current versus time plot obtained using the DC polarization technique, the resistance before and after polarization, and the obtained lithium transference number was tabulated in Table 3. The measured initial and steady-state currents were used to calculate the lithium transference number using Eqn (3) and included in Table 3. The lithium transference number obtained for SPE1 is 0.088, which is slightly lower than 0.16 reported by Xiao *et al.* for P(VDF-HFP)-$LiPF_6$-EC polymer electrolytes (Xiao, 2018). The low lithium transference number reported for SPE1 is associated with insufficient free Li^+ ions available for ionic conduction due to the formation of polymer-salt complexes.

However, with micron-sized Al_2O_3 and SiO_2 fillers in the polymer matrix, the lithium transference number increases up to 0.215 and 0.263 for SPE2 and SPE3, respectively. Xiao *et al.* reported similar findings in their studies where the incorporation of nano-sized inorganic fillers enhances the lithium transference number (Xiao, 2018). They obtained a lithium transference number of 0.28 to 0.41 at room temperature for P(VDF-HFP) polymer electrolytes with 5-15 wt% of nano PMMA-ZrO_2 particles, which is an improvement from 0.16 without nano PMMA-ZrO_2 particles. The improvement in lithium transference number is associated with the distribution of inorganic filler in the polymer matrix.

Firstly, the presence of inorganic fillers reduces the fraction of polymer-salt complexes as inorganic fillers such as Al_2O_3 and SiO_2 fillers also forms polymer-ceramic complexes with the polymer host. This means that there is more Li^+ ions will be available for ionic conduction. Besides that, inorganic fillers also promote amorphous region in the polymer matrix as they reduced the degree of crystallinity of the polymer chain by lowering the glass transition temperature, T_g, which in turn enhances the ionic mobility, thus leading to improved lithium transference number.

Table 4. Lithium transference number obtained in this work compared to other researchers.

Composition	Type	Reference	t^+
PMMA-$LiCF_3SO_3$-EC	Solid	This work	0.088
PMMA-$LiCF_3SO_3$-EC-Al_2O_3 (≤ 10μm)	Solid	This work	0.215
PMMA-$LiCF_3SO_3$-EC-SiO_2 (≤ 10μm)	Solid	This work	0.263
PMMA-$LiClO_4$-EC	Gel	Faridi [7]	0.39-0.42
PMMA-$LiPF_6$-EC	Gel	Musil [8]	0.24-0.69
PMMA-$LiClO_4$-PC-EC	Gel	Appetecchi [26]	0.40
PMMA-LiBOB-EC	Gel	Hosseinioun [9]	0.34
PEO-$LiCF_3SO_3$EC-SiO_2 (≤ 12nm)	Gel	Wang [27]	0.54
PEO-$LiBF_4$-EC-SiO_2 (≤ 12nm)	Gel	Liu [28]	0.34-0.56
P(VDF-HFP)-$LiPF_6$-EC-PMMA-ZrO_2	Solid	Xiao [15]	0.28

Table 4. shows the comparison for the lithium transference number obtained in this work to other literature. From the comparison, we can see that PMMA SPEs still have a lower lithium transference number compared to GPEs, as reported by (Faridi, 2018; Hosseinioun, 2019; Liu, 2004). This is acceptable because GPEs were much amorphous compared to SPEs due to their higher liquid solution. However, the higher liquid solution in GPEs results in a mechanically soft system and lower thermal stability. Although PMMA SPEs incorporated with inorganic fillers has lower lithium transference number compared to GPEs, but the presence of fillers in the polymer matrix served as a backbone for PMMA SPEs that ensure better mechanical and thermal stability compared to GPEs. Liang *et al.* show that the dispersion of nano-Al_2O_3 fillers into PEO-PMMA-LiTFSI polymer matrix enhances the tensile strength of SPEs up to 3.26 MPA compared to 2.78MPA for SPEs without inorganic filler (Liang, 2015).

Nevertheless, the lithium transference number in our study is comparable to the work from Xiao *et al.*. They reported lithium transference number ranging from 0.28 to 0.41 for P(VDF-HFP) polymer electrolytes doped with nano PMMA-ZrO_2 particles, close to 0.263 obtained for PMMA-$LiCF_3SO_3$-EC-SiO_2 in our study (Xiao, 2018). The lithium transference number in their study is higher than ours because they were using 5%-15% of nano PMMA-ZrO_2 particles while we only added 2% of SiO_2 fillers. Furthermore, the nano PMMA-ZrO_2 particles also have a greater effective surface area than micron-sized SiO_2 fillers, which also contributed to the higher lithium transference number obtained in their studies.

Figure 3. shows the LSV plot of the samples. The voltages were swept from 0V (versus stainless steel electrode) at a scan rate of 5 mVs^{-1} until a large increment of current was observed (see Figure 3). The large increment in current observed indicates the breakdown

of the electrolyte films. The stability voltage can be determined as the intersection of the extrapolated linear current in the high voltage region with the voltage axis.

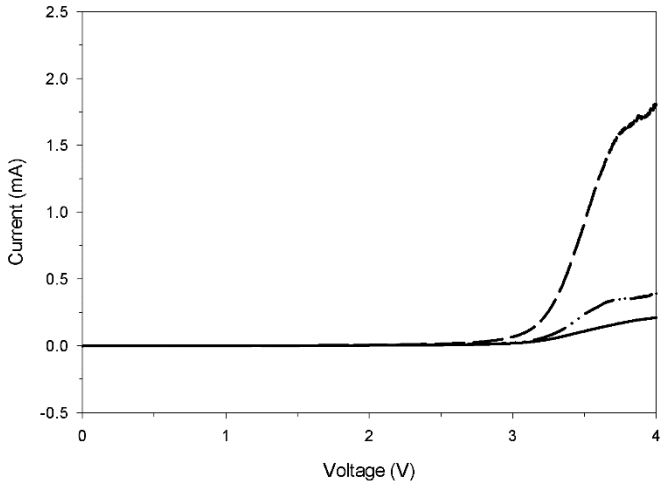

Figure 3. LSV curves with a scan rate of 5mVs^{-1} for PMMA-LiCF$_3$SO$_3$-EC (Solid line), (b) PMMA-LiCF$_3$SO$_3$-EC-Al$_2$O$_3$ (Dash dotted line), and PMMA-LiCF$_3$SO$_3$-EC-SiO$_2$ (Dash line).

LSV results revealed that the potential window of the blend is all above 3.0V; SPE1 (3.07V), SPE2 (3.13V), and SPE3 (3.2V). There was a notable improvement in the SPE voltage stability window containing inorganic filler compared to the polymer salts system. In comparison, Chandra *et al.* obtained an electrochemical stability voltage of 2.69V for PVC-PMMA-LiCl-TiO$_2$ polymer blend, an improvement from 1.69V without TiO$_2$ nanoparticles (Chandra, 2017). Dhatarwal *et al.* also reported stability of 3.0V for PEO-PMMA polymer blend doped with various nanoparticles (Dhatarwal, 2018).

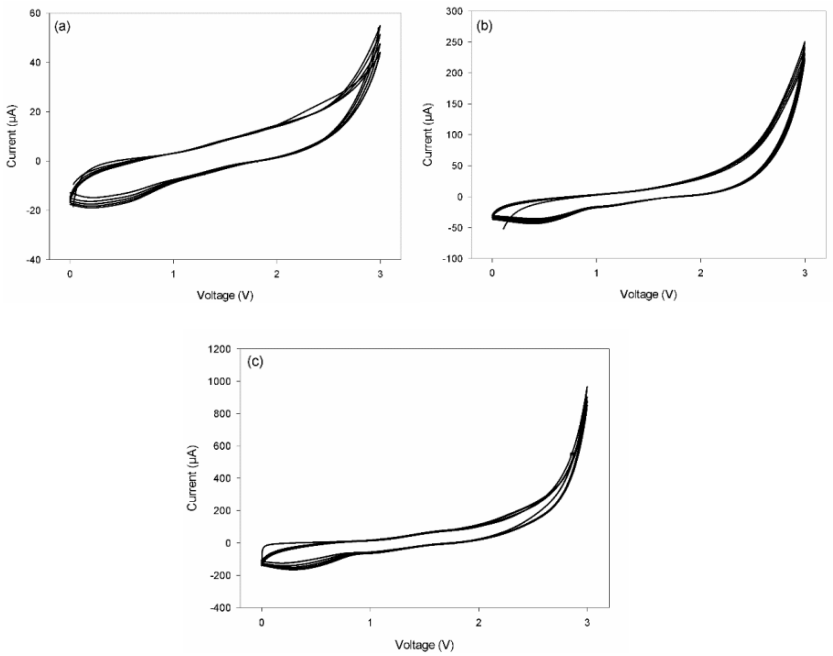

Figure 4. Five cycles of cyclic voltammetry curve versus stainless steel electrodes with a scan rate of 20mVs^{-1} for (a) PMMA-$LiCF_3SO_3$-EC, (b) PMMA-$LiCF_3SO_3$-EC-Al_2O_3 and (c) PMMA-$LiCF_3SO_3$-EC-SiO_2

The CV curve of the SPEs was shown in Figure 4. (see Figure 4). The absence of redox peak voltages and the overlapping of the subsequent sweeps indicates that the charging and discharging reaction at the interface between the electrolytes film and stainless-steel electrode is fully reversible for all the SPE films tested (Bandarayake, 2015). Jinisha *et al.* reported CV curve of a similar shape for PEO/PVP-$LiNO_3$ SPEs in their studies (Jinisha, 2017). They explained that the missing oxidation-reduction peaks in CV curves suggested that the SPE film has great reversibility within the voltage range. Furthermore, Bandarayake *et al.* also reported that CV curves with subsequent overlapping sweeps show that the SPE has good cycling capability and a longer lifetime. Their samples can retain 96% of its original specific capacity after 20 cycles (Bandarayake, 2016).

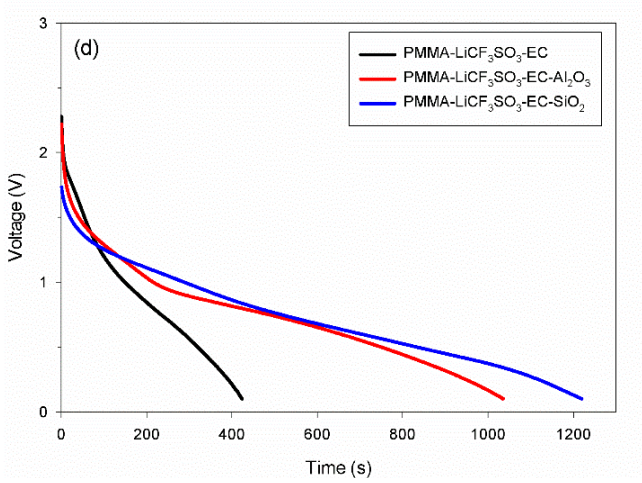

Figure 5. Discharge curve with a discharge current of 0.01mA for PMMA-$LiCF_3SO_3$-EC (black line), PMMA-$LiCF_3SO_3$-EC-Al_2O_3 (red line) and PMMA-$LiCF_3SO_3$-EC-SiO_2 (blue line) versus stainless steel electrodes

Furthermore, PMMA-$LiCF_3SO_3$-EC-SiO_2 that were doped with SiO_2 fillers samples has the highest energy density as evidenced by the discharging time as presented in Figure 5. (see Figure 5). It can be seen that PMMA-$LiCF_3SO_3$-EC-SiO_2 takes approximately 16% and 190% longer time to discharge compared to PMMA-$LiCF_3SO_3$-EC-Al_2O_3 and PMMA-$LiCF_3SO_3$-EC, respectively.

4.0 CONCLUSIONS

This work provided the ionic conductivity, lithium transference number, and electrochemical performance of PMMA SPEs. SiO_2 fillers enhanced PMMA SPEs can exhibit ionic conductivity of 2.35×10^{-4} S/cm and lithium transference number of 0.263 at room temperature. It is suggested that inorganic fillers promote amorphous region in PMMA SPEs, and the greater effective area of the fillers also provides pathways for ionic conduction. Besides, the presence of inorganic fillers reduces the fraction of polymer-salt complexes, freeing more Li^+ ions for ionic conduction. The electrochemical studies also show that inorganic filler enhanced PMMA SPEs has great cycling capability and

reversibility within a voltage range of 3.0V. Inorganic filler enhanced SPEs may not exhibit superb ionic conductivity and lithium transference number like GPEs, but they had better mechanical and thermal properties than GPEs, which made SPEs much suitable for lower energy density but higher safety applications.

5.0 ACKNOWLEDGEMENT

This work is supported by FRGS/2019, Ministry of Higher Education, Malaysia.

6.0 REFERENCES

Appetecchi, G. B., Croce, F., & Scrosati, B. (1997). High-performance electrolyte membranes for plastic lithium batteries. *J. Power Sources*, 66(1–2), 77–82.

Aziz, S., Abdulwahid, R., & Hamsan, M. (2019). Proton Conducting Chitosan-Based Polymer Blend Electrolytes with High Electrochemical Stability. *Molecules*, vol. 24, pp. 1–15, 2019.

Bandara, L. R. A. K., Dissanayake, M. A. K. L., & Mellander, B. (1998). Ionic Conductivity of Plasticized (PEO)-$LiCF_3SO_3$ electrolytes. *Electrochimica Acta*., vol. 43, 1447-1451.

Bandaranayake, C. M., Weerasinghe, W. A. D. S. S., Vidanapathirana, K. P. (2016). A Cyclic Voltammetry study of a gel polymer electrolyte based redox-capacitor. *Sri Lankan J. Phys.*, 16(1), 19-27.

Chandra, M. V. L., Karthikeyan, S., & Selvasekarapandian, S. (2017). Study of PVAc-PMMA-LiCl Polymer Blend Electrolyte and the Effect of Plasticizer Ethylene Carbonate and Nanofiller Titania on PVAc-PMMA-LiCl Polymer Blend Electrolyte. *J. Polym. Eng.*, 37(6), 617–631.

Chauvin, C., Alloin, F., Judeinstein, P., & Foscallo, D. (2006). Electrochemical and NMR Characterizations of Mixed Polymer Electrolytes Based on Oligoether Sulfate and Imide Salts. *Electrochim. Acta*, 52(3), 1240–1246.

Chew, K. W., & Tan, K. W. (2011). The Effects of Ceramic Fillers on PMMA-based Polymer Electrolyte Salted with Lithium Triflate, $LiCF_3SO_3$. *Int. J. Electrochem. Sci.*, 6(11), 5792–5801.

Dhatarwal, P., Choudhary, S., & Sengwa, R. J. (2018). Electrochemical Performance of Li^+ Ion Conducting Solid Polymer Electrolytes Based on PEO–PMMA Blend Matrix Incorporated with Various Inorganic Nanoparticles for the Lithium Ion Batteries, *Compos. Commun.*, 10, 11–17.

Ding, Z., Li, J., & An, C. (2020). Review—Interfaces: Key Issue to Be Solved for All Solid-State Lithium Battery Technologies. *J. Electrochem. Soc.*, 167(7), 070541.

Dissanayake, M. A. K. L., Jayathilaka, P. A. R. D., Bokalawala, R. S. P. & Albinsson, I. (2003). Effect of Concentration and Grain size of Alumina Filler on the Ionic Conductivity Enhancement of the $(PEO)_9LiCF_3SO_3$:Al_2O_3 Composite Polymer Electrolyte. *J. Power Sources*, 119–121, 409–414.

Evans, J., Vincent, C. A., & Bruce, P. G. (1987). Electrochemical Measurement of Transference Numbers in Polymer Electrolytes. *Polymer (Guildf).*, 28(13), 2324–2328.

Faridi, M., Naji, L., Kazemifard, S., & Pourali, N. (2018). Electrochemical Investigation of Gel Polymer Electrolytes Based on Poly (methyl methacrylate) and Dimethylacetamide for Application in Li-Ion Batteries. *Chem. Pap.*, 72(9), 2289–2300.

Hosseinioun, A., Nürnberg, P., Schönhoff, M., & Diddens, D. (2019). Improved Lithium Ion Dynamics in Crosslinked PMMA Gel Polymer Electrolyte. *RSC Adv.*, 9(47), 27574–27582.

Jiang, Z., Han, Q., Wang, S., & Wang, H. (2019). Reducing the Interfacial Resistance in All-Solid-State Lithium Batteries Based on Oxide Ceramic Electrolytes. *ChemElectroChem*, 6(12), 2970–2983.

Jinisha, B., Manoj, M., & Pradeep, P. (2017). Development of a Novel Type of Solid Polymer Electrolyte for Solid State Lithium Battery Applications Based on Lithium Enriched Poly (ethylene oxide) (PEO)/poly (vinyl pyrrolidone) (PVP) Blend Polymer. *Electrochim. Acta*, 235, 210–222.

Kurapati, S., Gunturi, S. S., Nadella, K. J., & Erothu, H. (2019). Novel Solid Polymer Electrolyte Based on PMMA:CH_3COOLi Effect of Salt Concentration on Optical and Conductivity Studies. *Polym. Bull.*, 76(10), 5463–5481.

Liang, B., Tang, S., Jiang, Q., & Chen, C. (2015). Preparation and Characterization of PEO-PMMA Polymer Composite Electrolytes Doped with Nano-Al_2O_3. *Electrochim. Acta*, 169, 334–341.

Lim, Y. S., Jung, H. A., & Hwang, H. (2018). Fabrication of PEO-PMMA-$LiClO_4$-Based Solid Polymer Electrolytes Containing Silica Aerogel Particles for All-Solid-State Lithium Batteries. *Energies*, 11(10), 2559.

Liu, Y., Lee, J. Y., & Hong, L. (2004). In Situ Preparation of Poly (ethylene oxide)-SiO_2 Composite Polymer Electrolytes. *J. Power Sources*, 129(2), 303–311.

Marcinek, M., Bac, A., & Lipka, P. (2000). Effect of Filler Surface Group on Ionic Interactions in PEG-$LiClO_4$-Al_2O_3 Composite Polyether Electrolytes. *J. Phys. Chem. B*, 104(47), 11088–11093.

Musil, M., & Vondrak, J. (2014). Transference Number Measurements on Gel Polymer Electrolytes for Lithium-Ion Batteries. *ECS Transactions*, 63(1), 315-319.

Osińska, M., Walkowiak, M., & Zalewska, A. (2009). Study of the role of ceramic filler in composite gel electrolytes based on microporous polymer membranes. *J. Memb. Sci.*, vol. 326, no. 2, pp. 582–588.

Pal, P., & Ghosh, A. (2018). Investigation of Ionic Conductivity and Relaxation in Plasticized PMMA-$LiClO_4$ Solid Polymer Electrolytes. *Solid State Ionics*, 319, 117–124.

Pitawala, H. M. J. C., Dissanayake, M. A. K. L. & Seneviratne, V. A., (2007). Combined Effect of Al_2O_3 Nano-Fillers and EC Plasticizer on Ionic Conductivity Enhancement in the Solid Polymer Electrolyte $(PEO)_9LiTf$. *Solid State Ionics*, 178(13–14), 885–888.

Pożyczka, K., Marzantowicz, M., Dygas, J. R. & Krok, F. (2017). Ionic Conductivity and Lithium Transference Number of Poly (ethylene oxide): LiTFSI system. *Electrochim. Acta*, 227, 127–135.

Saikia, D., Chen, Y. T., Li, Y. K., & Lin, S. I. (2008). Investigation of Ionic Conductivity of Composite Gel Polymer Electrolyte Membranes Based on P(VDF-HFP), $LiClO_4$ and Silica Aerogel for Lithium-Ion Battery. *Desalination*, 234(1–3), 24–32.

Sivakumar, P., & Gunasekaran, M. (2015). Highly Porous Polymer Electrolytes Based on P(VDF-HFP)/ PEMA with Propylene Carbonate/Diethyl Carbonate for Lithium Battery Applications. *Int. J. Energy Power Eng. Int. J. Energy Power Eng. Spec. Issue Energy Syst. Dev.*, 4(5), 17–21.

Song, C., Xu, C., & Chen, Y. (2015). Enhanced Thermal and Electrochemical Properties of PVDF-HFP/PMMA Polymer Electrolyte by TiO_2 nanoparticles. *Solid State Ionics*, 282, 31–36.

Sun, C. C., You, A. H., & Teo, L. L. (2019). Characterizations of PMMA-based Polymer Electrolyte Membranes with Al_2O_3. *J. Polym. Eng.*, 39(7), 612–619.

Wang, W. & Alexandridis, P. (2016). Composite Polymer Electrolytes: Nanoparticles Affect Structure and Properties. *Polymers (Basel).*, 8(11), 387.

Xiao, W., Wang, Z., & Zhang, Y. (2017). Enhanced Performance of P(VDF-HFP)-Based Composite Polymer Electrolytes Doped with Organic-Inorganic Hybrid Particles PMMA-ZrO_2 for Lithium Ion Batteries. *J. Power Sources*, 382, 128–134.

Yang, J., Wang, X., Zhang, G., Ma, A., & Chen, W. (2019). High-Performance Solid Composite Polymer Electrolyte for all Solid-State Lithium Battery Through Facile Microstructure Regulation. *Front. Chem.*, 7, 1–11.

Yao, P., Yu, H., & Ding, Z. (2009). Review on Polymer-Based Composite Electrolytes for Lithium Batteries. *Front. Chem.*, 7, 1–17.

Zakariya'u, I., Gultekin, B., Singh, V. (2020). Electrochemical Double-Layer Supercapacitor using Poly(methyl methacrylate) Solid Polymer Electrolyte. *High Perform. Polym.* 32(2), 201–207.